Study of the capability of energy dispersive small angle x-ray scattering with synchrotron radiation

Kuan-Li Yu
Department of Engineering and System Science, National Tsing Hua University, Hsinchu, Taiwan 300, Republic of China

Chih-Hao Lee[a)]
Department of Engineering and System Science, National Tsing Hua University, and Synchrotron Radiation Research Center, Hsinchu, Taiwan 300, Republic of China

Ching-Shiang Hwang
Synchrotron Radiation Research Center, Hsinchu, Taiwan 300, Republic of China

Huan-Chi Tseng
Department of Engineering and System Science, National Tsing Hua University, Hsinchu, Taiwan 300, Republic of China

Poh-Kun Tseng
Synchrotron Radiation Research Center, Hsinchu, Taiwan 300 and Department of Physics, Tamkang University, Tamsui, Taiwan 251, Republic of China

Tsang-Lang Lin
Department of Engineering and System Science, National Tsing Hua University, Hsinchu, Taiwan 300, Republic of China

Szu-Li Chang
Department of Nuclear Science, National Tsing Hua University, Hsinchu, Taiwan 300, Republic of China

Rong-Jiun Sheu
Department of Engineering and System Science, National Tsing Hua University, Hsinchu and Synchrotron Radiation Research Center, Hsinchu, Taiwan 300, Republic of China

Sow-Hsin Chen
Department of Nuclear Engineering, Massachusetts Institute of Technology, Cambridge, Massachusetts 02139

(Received 29 September 1998; accepted for publication 4 May 1999)

Energy dispersive small angle x-ray scattering is a unique method that takes advantage of a continuous spectrum of a synchrotron radiation source. In this study, the capability of this scattering measurement is explored. Using a detector mask with three acceptance rings of different ring radius and a sample to detector distance of 440 mm with the usable x-ray energy ranging from 4 to 20 keV, we can cover a q range from 0.01 to 0.4 $Å^{-1}$. However, sample transmission and detector response function limit the application range at low energy. Slit scattering is the dominant source of background. The signal to background ratio for a standard cross-linked polyethylene sample can be more than 100. For a time-resolved experiment, data acquisition rate is limited by the throughput of the detector. © *1999 American Institute of Physics.* [S0034-6748(99)03508-X]

I. INTRODUCTION

In a conventional small angle x-ray scattering (SAXS) experiment, one can measure the scattering profile with a monochromatic x ray as a function of scattering angle. On the contrary, in the energy dispersive small angle x-ray scattering (EDSAXS) experiment, one can measure the scattering profile as a function of scattered x-ray energy at a fixed scattering angle with a polychromatic x-ray source in conjunction with an energy-dispersive detector. Since in an EDSAXS method, all the photons with different energies are registered at the detector, it could be used to study the time-dependent phenomena such as kinetics of phase separation, morphological transformation, sol–gel process, and the synthesis of other advanced materials. Pioneering studies have been done by Schultz and Long[1] and Bordas and Munro[2,3] by using the synchrotron radiation. However, detailed description of this method was not fully illustrated. In this study, we mainly describe the setup of our EDSAXS spectrometer and the conversion of a raw EDSAXS spectrum into a useful data. Furthermore, the importance of obtaining various correction factors to get a true sample scattering profile and the procedures to eliminate the background are emphasized. The capability and the limitation of this method are also discussed in the later sections.

II. EXPERIMENTAL SETUP

EDSAXS experiments were performed at the bending magnet BL20B beamline at Synchrotron Radiation Research

[a)]Electronic mail: chlee@ne.nthu.edu.tw

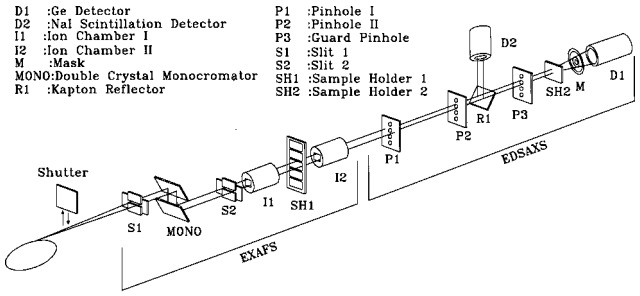

FIG. 1. Schematic BL20B beamline setup.

Center (SRRC). The BL20B beamline is a multipurpose beamline for x-ray spectroscopy, x-ray imaging, x-ray scattering and instrumentation test.[4] Figure 1 shows a schematic drawing of the BL20B beamline. Since there is no mirror in this beamline, high energy synchrotron photons are fully available without suffering from the high energy cutoff due to the mirror reflection. The continuous spectrum (white beam) of the synchrotron radiation was used in the EDSAXS experiments, where the monochromatic beam was to calibrate the sample transmission and detector response functions. A position sensitive splitting ion chamber, which is a design similar to that of Schildkamp and Pradervand,[5] was used to monitor the beam position and intensity throughout the experiments.

The EDSAXS section of the BL20B beamline consists of a three-pinhole system to collimate the incident x rays, a detector mask to define the scattering angle, and a large area ORTEC LO-AX Ge detector to collect the scattered photons of different energies. The detector mask (see Fig. 2) consists of three photon acceptance rings to define three different ranges of scattering vectors q. By using an acceptance ring selector that is placed in front of the detector mask rings, we can select one specified ring at a time to collect the energy dispersive data. A detailed description of each major component follows.

A. Three-pinhole system and intensity monitor

This three-pinhole system consists of the collimating pinholes (pinholes I, II) and the guard pinhole (pinhole III). Each pinhole was made of a 1 mm thick Ta sheet with four different pinhole sizes, and mounted on an X-Z stage. One can select the size and position of the pinhole by moving the X-Z stage during alignment. The collimating pinholes that are separated by a distance of 2 m were used to define the incident beam divergence of x rays. The purpose of the guard pinhole is to eliminate the stray scattered x rays from the collimating pinholes.

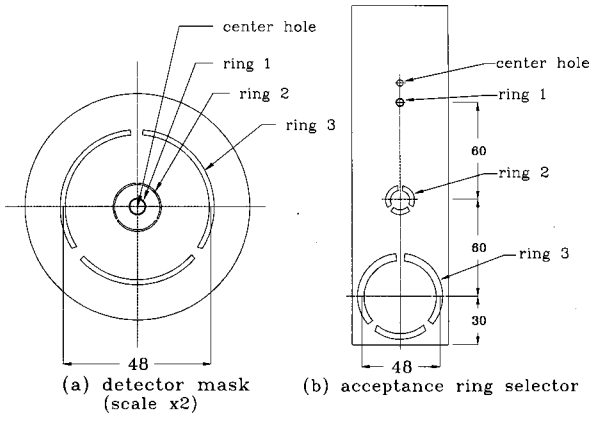

FIG. 2. The design of detector mask and acceptance ring selector.

TABLE I. The measurable q range as a function of sample-to-mask distance (SMD) and acceptance ring diameters with energy range of 4–20 keV.

Acceptance ring diameter (mm)	Ring width (mm)	SMD 440 mm ($Å^{-1}$)	SMD 1550 mm ($Å^{-1}$)	SMD 4400 mm $Å^{-1}$
4.7	0.15	0.01–0.04	0.003–0.012	0.0011–0.004
15	0.48	0.035–0.13	0.01–0.037	0.0034–0.013
48	1.55	0.11–0.42	0.03–0.12	0.011–0.041

A NaI(T1) scintillation detector and a 25 μm Kapton foil, which is placed 45° to the incident beam to reflect a small portion of the beam to the detector, served as a photon flux monitor to track the variation of intensity of the incident x rays. The photon flux monitor is positioned after the collimating pinholes, so that, a slight electron orbit shift can be monitored by sensing an intensity drop in the NaI(T1) detector.

B. Detector mask system

The design of the detector mask system is shown in Fig. 2. It consists of two components: (a) a detector mask to define the scattering angles; (b) an acceptance ring selector to select the desired angle. The detector mask, which has three concentric circular rings with diameters of 4.7, 15, and 48 mm, respectively, was mounted on an X-Z stage for easy alignment. At the center of this mask, a 0.2 mm center pinhole was prepared, so that the detector mask could be positioned to the direct beam within 0.05 mm of accuracy. The acceptance ring selector, which has four different patterns of accessible holes, was mounted on a Z-motion linear stage and placed in front of the detector mask. By selecting the Z position of this ring selector, only one of the acceptance rings or the center alignment pinhole on the detector mask is chosen. Since we want to collect as many scattering photons as possible at a fixed angle, the acceptance ring selector was used instead of a defining slit. The resulting range of the scattering vector q is 0.001–0.4 $Å^{-1}$ for the incident energy from 4 to 20 keV and the sample-to-mask distance (SMD) switched among 440, 1550, and 4400 mm (see Table I). However, it is much easier to change the measurement range by selecting the acceptance ring than changing the SMD during the experiment.

C. Alignment and collimation

Alignment is the most important factor in determining the accuracy of a SAXS experiment. The alignment procedures are: (1) to align the three-pinhole system; (2) to align the LO-AX detector to the collimated beam; (3) to center the detector mask to the beam and then set the mask selector to the desired ring for experiment.

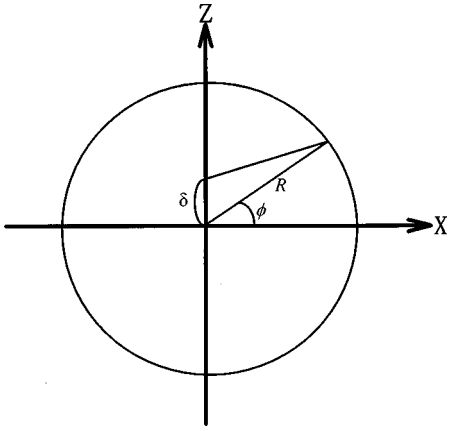

FIG. 3. The calculation of misalignment effect of the acceptance rings.

In order to align the whole EDSAXS system, all the pinholes and acceptance ring selector are coated with P-43 phosphor powder for visible alignment through viewports. In the first step of alignment, we usually align the first pinhole with the other pinholes wide opened. After the first pinhole has been aligned, the next downstream pinhole was then aligned. It is important to note that the diameter of the following pinhole should be slightly larger than the previous one. Therefore, the parasitic scattering from the previous pinhole would be eliminated. The alignment of the three pinholes should be accurate within 0.02 mm, which is comparable to the vertical size of the electron bunch in the storage ring, relative to the electron orbit plane. If the pinhole was placed out of the orbit plane, the spectrum of the incoming synchrotron radiation will be softer due to the fact that the higher energy photons are emitted within a smaller divergent angle of a synchrotron radiation source.

To align the LO-AX detector, an aligned 0.2 mm pinhole was placed at the center in front of the detector. The detector was then aligned by scanning the X-Z stage attached to the detector. The accuracy of detector alignment is not crucial because the diameter of the Ge crystal in the LO-AX detector is 51 mm, which is larger than the largest diameter of the acceptance ring. During this alignment procedure, a 3 mm aluminum attenuator was placed at the upstream of the detector to prevent the counting rate of the detector system saturated by the direct beam.

After the detector and three incident pinholes were positioned, the detector mask was aligned with the collimated beam by scanning the 0.2 mm center pinhole on the detector mask. Unlike the alignment of detector and acceptance ring selector, the mask should be aligned precisely in order to determine the scattering vector q accurately. The effect of misalignment can be given by (see Fig. 3):

$$q(\phi)\approx 2\pi\left(\frac{\sqrt{R^2+\delta^2-2R\delta\cos\left(\frac{\pi}{2}-\phi\right)}}{L\lambda}\right), \qquad (1)$$

$$q(\phi)=(2\pi/\lambda)(R/L)(1-\delta\sin\phi/R) \qquad \text{if} \quad \delta\ll R, \quad (2)$$

where R is the radius of the acceptance ring on the detector mask δ is the misaligned distance from the center, L is the SMD, and ϕ is the azimuthal angle. For an isotropic system, we integrate all the ϕ angles to get the q broadening. For example, in our experiment, the SMD is 440 mm and the acceptance ring diameter is 4.7 mm, if the offset of the beam center to mask center is 1 mm, the fractional standard deviation in the broadened q distribution will be 14.8%. If the alignment can be achieved within 0.05 mm, the fractional standard deviation could be reduced to an acceptable value of 0.75%. Finally, the acceptance ring selector was positioned to select only one of the acceptance rings on the detector mask to define the scattering angle.

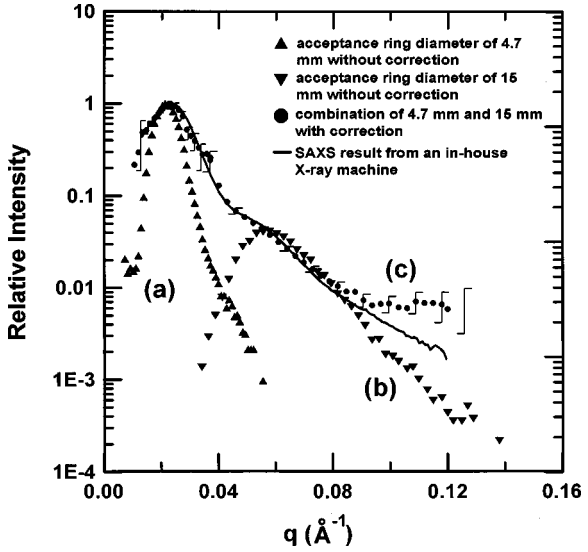

FIG. 4. The scattering profile of a standard cross-linked polyethylene sample. (a) The measured scattering profile with acceptance ring of 4.7 mm diameter without correction. (b) The measured scattering profile with acceptance ring of 15 mm diameter without correction. (c) The corrected EDSAXS scattering profile. The solid line is the experimental result from a 10 m SAXS facility with 18 kW rotating anode x-ray machine.

To eliminate the scattering background, two apertures were positioned after the sample chamber. The first one was placed between the sample and the detector mask and the second one between the mask and the entrance of the Ge detector. The diameter of the aperture was selected to limit the scattered photons from the wall of upstream vacuum pipe to reach the area of downstream components. In this way, the background scattering from the chamber wall can be reduced by half. Furthermore, fluorescence background can be significantly reduced by lining the stainless steel vacuum chamber with a 0.4 mm aluminum sheet.

III. MEASUREMENTS OF A STANDARD SAMPLE

A cross-linked polyethylene was used as a standard sample to test the performance of this EDSAXS spectrometer. Two different diameters of the acceptance rings were used on the detector mask at the SMD of 440 mm. The measured intensity distributions are shown in Fig. 4. Solid triangles [curve (a)] and reversed triangles [curve (b)] are the measured results without correction of the 4.7 and 15 mm acceptance ring, respectively. Solid dots [curve (c)] depict the corrected scattering spectrum, which is the combination of the normalized (a) and (b) with correction. The scattering profile of this sample was also measured at a conventional 10 m SAXS spectrometer in the X-ray Laboratory of the De-

partment of Engineering and System Science, National Tsing Hua University. The measured intensity distribution is the solid line in Fig. 4.

The SAXS intensity $I(E')$ measured by the EDSAXS spectrometer can be given as

$$I(E')=\int_{E'}^{\infty} I_0(E)\times T_{mW}(E)\times\{[\sigma_S(E)\times N\times t+S(E)]\times T_{mS}(E)+F(E)\}\times T_{mD}(E)\times E_R(E',E)dE, \tag{3}$$

where $I_0(E)$ is the white beam spectrum of synchrotron radiation, $T_{mW}(E)$ is the transmission factor of windows in the beamline, $T_{mS}(E)$ is the transmission factor of the sample, $T_{mD}(E)$ is the transmission factor of the Be window of the detector, $\sigma_S(E)$ is the scattering cross section of the sample, $S(E)$ is the intensity of the parasitic scattering from pinhole edges before the sample chamber, $F(E)$ is the fluorescence intensity after the sample chamber, $E_R(E',E)$ is the detector response function (including the detector efficiency) at energy E' due to the incident photons at energy E, N is the atomic density of the sample, and t is the thickness of the sample,

To obtain the true SAXS intensity $\sigma_S(E)$, the following corrections have to be considered:

(1) Subtract the background scattering from the empty sample cell, windows, and pinhole edges.
(2) Corrections of the detector response functions, i.e., subtract the low energy tail and Ge K_α, K_β escape peaks in the detected spectrum by the stripping method.
(3) Correct for the absorption due to the Be windows and Kapton windows in the beamline and the window of the Ge detector.
(4) Correct for the absorption of the sample holder and sample itself.
(5) Normalize to the spectrum of synchrotron radiation from the bending magnet.

We will discuss the correction factors in detail in this section.

A. Background measurement

The major background contribution is the parasitic scattering from the upstream pinholes. Since the second pinhole only intersects the parasitic photons from the first pinhole, the amount of pinhole scattering from the edge of the second pinhole will be much smaller. However, a typical misalignment of the second pinhole or a drift of electron orbit will cause the edge of the second pinhole to intersect with the collimated direct beam from the first pinhole. In this case, the intensity of parasitic scattering from pinholes will increase by 2 to 3 orders of magnitude. As we have mentioned in Sec. II, in order to eliminate the parasitic scattering from the edge of the upstream pinholes, the diameter of each pinhole was selected carefully. The diameter of the second pinhole is slightly larger than the previous pinhole and the diameter of the guard pinhole is again larger than the upstream pinholes. Figure 5 shows a comparison of background with

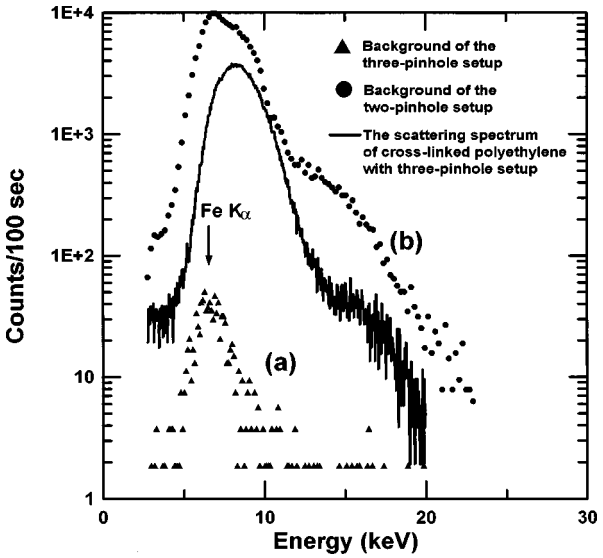

FIG. 5. The result of background measurement using different pinhole settings: (a) The three pinhole setup with pinhole diameters of 0.21, 0.25, and 0.6 mm for pinholes I, II and guard pinhole, respectively; (b) the two-pinhole setup with the same pinhole sizes, 0.21 and 0.25 mm of pinholes I and II, respectively. The solid line is the scattering spectrum of cross-linked polyethylene with the three-pinhole setup.

different pinhole setting. Solid triangles [curve (a)] are the measured background with only the pinhole diameters of 0.21, 0.25, and 0.6 mm for pinholes I, II, and the guard pinhole, respectively. Solid dots [curve (b)] are the background with only the first two pinholes of the same setting as in (a), where the guard pinhole was kept wide open (diameter of 2.2 mm). It can be shown that the background could be reduced by about 100-fold, if one chose a good pinhole setting. The measured spectrum of cross-linked polyethylene before correction with the same pinhole setting of (a) is also shown in Fig. 5 (solid line). The intensity of the background with only two pinholes (solid dots) is even about ten times larger than the scattering intensity of the sample with a three-pinhole setup. When the background contribution from the parasitic scattering from the edge of the upstream pinhole was almost totally eliminated, the residual background [curve (a) in Fig. 5] looks like the fluorescence photons induced by direct and scattered x rays. This fluorescence background is the characteristic x ray of Fe, Ni, and Co, which might come from the surrounding detector materials because we have put a 0.4 mm thick Al lining on the surface of the steel vacuum chamber already.

To do the background correction of the sample is not straightforward. If the background is the scattering photons from the upstream vacuum pipes, the background should be subtracted after multiplying the sample transmission function. If the background is attributed to the induced fluorescence photons after the detector mask, the background subtraction depends on the energy of the incoming photons, and the correction procedure is very complicated. If the incoming photon energy is higher than the absorption edge of surrounding materials, the fluorescence background should be considered. Fortunately, the background is small compared to the scattering intensity of the sample after a good alignment. The background correction has little effect as long as

the background intensity is sufficiently small compared with the sample scattering.

B. Detector response function and efficiency calibration

The response function of the ORTEC LO-AX Ge detector is measured by using ^{55}Fe, ^{241}Am sources and monochromatic synchrotron radiation. The efficiency of the detector as a function of the incident x-ray energy is also calibrated within 5% of accuracy against a scintillation detector and an ion chamber by using a Kapton foil sample. The detector response functions and the efficiencies across the area of the Ge detector are also measured by putting a pinhole before the detector at different detector positions. The response functions and efficiencies of x-ray energies below 25 keV for three different acceptance rings are similar within a 5% difference.

The signal output of this Ge detector is quite small and is acoustic sensitive because of its large input capacitance and large crystal size. The typical amplifier output is smaller than 0.5 V (for ^{55}Fe 5.9 keV) at an amplifier (ORTEC 573) gain of 1000. A small acoustic vibration on this beamline gives rise to a best energy resolution of only 450 eV (at 5.9 keV) compared to the specification of 350 eV. However, the detector energy resolution is not a dominant factor in determining the SAXS profile in our measurement.

C. Detector response function correction

In the detector calibration, we found that the monoenergetic response of the detector consists of a long low energy tail, which is due to either an incomplete charge collection[6,7] or a Compton scattering. A significant Ge escape peak was also found when the incident x-ray energy is higher than 11.23 keV. The intensity ratio of the escape peak to the full energy peak is more important than the incomplete charge collection effect at high incident photon energies. A stripping program was written to eliminate the long low energy tail component and the Ge escape peak. Although the stripping method was known to have a large cumulative error at the low energy part in the unfolding processes of neutron or gamma ray spectra, that problem is not as serious in our x-ray measurement because the low energy tail is small enough. In fact, from the measured spectrum before correction, we can see a step at the low energy part of the spectrum [$E<4$ keV in curve (c) of Fig. 5] which is the cumulative tail components due to the higher incident photons. After stripping, this low energy component can be totally eliminated.

D. Sample transmission measurement

The method of measuring the sample transmission is to place the detector 90 ° to the incident beam and measure only the scattering photon from a Kapton foil to avoid the Ge detector from saturation. The transmission coefficient as a function of energy was obtained by comparing the spectra measured with and without the sample in position. These two measured spectra should be corrected by the stripping method before further processing. Furthermore, special attention should be paid to reduce the background. For example, a cuplike beam stop placed at the end of the direct beam can reduce the fluorescence photon by at least 1 order of magnitude. A collimating pipe placed before the detector to accept only the scattering photon emitted from the position where the direct beam hit the Kapton foil can reduce several folds of background intensity.

E. White beam spectrum measurement

The white beam spectrum was obtained by measuring the scattering photon of direct beam with a Kapton foil, and was compared with the calculated spectrum of the bending magnet of the SRRC storage ring. In comparison, we can clearly see an intensity dip at 11.23 keV in the measured spectrum, which is the K edge of Ge. At the low energy part of the measured spectrum, the intensity was reduced a lot due to the absorption of Be and Kapton windows. The measured white beam spectrum was corrected with background, and then used to normalize the experimental data. In this normalization, the correction of absorption due to Be and Kapton windows, and the energy dependent detector efficiencies were cancelled out automatically.

F. The overall q resolution

The resolution function in the scattering vector can be roughly expressed by

$$\Delta q/q=[(\Delta\theta/\theta)^2+(\Delta E/E)^2]^{1/2}. \tag{4}$$

The resolution function consists of two components: the angular resolution of the setup and the energy resolution of the detector. The detector energy resolution is energy dependent, and can be expressed as $\Delta E/E=(N^2+2E)^{1/2}$, where N denotes the electronics noise. Since the electronic noise is the dominant factor in our experimental environment, a constant 8% of energy resolution was used for the energy range of 4–20 keV. The angular resolution is independent of energy. It depends on: (1) the ratio of ring width of the detector mask to the SMD; (2) the ratio of beam size to the SMD; and (3) the accuracy of the beam center to the mask center. All of these factors are convoluted into the angular uncertainty. The ring width is designed as wide as possible in order to accept more scattering photons under a reasonable q resolution. In this experimental setup, the ring width is 0.15–0.55 mm (see Table I). The corresponding $\Delta\theta/\theta$ is about 5%, which is comparable to detector energy resolution.

Since our measured scattering profile of the cross-linked polyethylene is quite smooth, the deconvolution process of the q resolution is not important. In fact, the q resolution in this experiment is very similar to a typical small angle neutron scattering setup with a velocity selector. Therefore, the correction is not necessary for this sample.

G. Final corrected result

After the measured spectrum is corrected for the background, the response function of the detector, and sample transmission, the resulting spectrum is then normalized by the white beam spectrum to obtain the corrected sample scattering profile which is shown in curve (c) of Fig. 4. The measured spectrum after correction can be compared with

the one measured with the conventional SAXS setup (the solid line in Fig. 4). The result is in good agreement with each other. The peak position at $q_{peak}=0.022\ \text{Å}^{-1}$ is identical in both scattering profiles. This result means that the EDSAXS method is a practical tool when proper correction and normalization procedures are used. Moreover, the data collection time to achieve the same counting statistic of EDSAXS is only 1 min, which is 50 times faster than that of a 10 m SAXS setup with a rotating anode x-ray machine.

IV. DISCUSSION

In EDSAXS measurement, there are many correction factors needed to be considered. Even when all the correction factors are taken into account, the experimental result still depends on the thickness and composition of samples because the sample transmission is different. For a thick sample, the energy spectrum measured at low energy range is not accurate because the penetration of the low energy x-rays through the sample is low, which also magnifies the error bars after the stripping method. Therefore, it is not adequate to do the Guinier plot (in which the low q part is usually emphasized) of the EDSAXS scattering profiles of thick samples. It is better to choose a large SMD (small $\sin\theta$) in the case of the thick sample so that higher energy part of spectrum (small λ) can still be applicable at the interested low q range.

On the other extreme, the EDSAXS result at the high q range, in which the Porod's plot is interested, should also be noted. For example, the stability of the beam position and beam incident angle of the incident beam should be monitored through the experiment, because the spectrum of synchrotron radiation is heavily angle dependent, especially at the high energy part. Another problem is the pileup or sum-peak effect. Usually, the dead time of the detector were kept below 10% in order to avoid the pileup effect at high q. And the sum-peak effect is especially important for a synchrotron radiation with a pulse type source.[8] The highest counting rate of the detector is kept below 4×10^4 cps by selecting the pinhole size. In a comparison of the experimental results of EDSAXS (solid dots in Fig. 4) and the conventional SAXS (solid line in Fig. 4), we can see that the scattering profile of EDSAXS is slightly higher than that of the conventional SAXS experiment for $q>0.09\ \text{Å}^{-1}$. This might be attributed to the pileup phenomena of the detection system.

Since the EDSAXS technique fully utilizes all the photons of the synchrotron spectrum, it is possible to do kinetics studies of some specific samples. In a kinetics study, the correction factors stated above were determined before and after the time-resolved experiments. During the experiment, we only need to monitor the change of the time-resolved spectra as the time evolved. Assuming the highest counting rate is 4×10^4 cps and an EDSAXS spectrum of 100 channels on a multichannel analyzer (MCA) is collected, the maximum collection time to get the time-resolved information is 10 s per spectrum. Although the rate of data acquisition is not as quick as a modern time-resolved SAXS experiment using an expensive charge coupled device detector, it still opens up an opportunity for a low cost setup to study a sample in time-resolved fashion. Improvement of the data acquisition rate can be done by using shorter shaping time and a flash type analog to digital converter with a sacrifice of energy resolution. By using a multielement detector, we can also improve the data acquisition rate, which has long been used in the x-ray absorption spectroscopy. With ten identical Ge crystals arranged in a circular array, the maximum detector throughput can be increased by a factor of 10. However, the cost of ten sets of preamplifiers, amplifiers, discriminators and MCAs is still very expensive today.

As a final note, this setup of concentric acceptance rings on the detector mask is only applicable to an isotropic scattering sample. For an anisotropic scattering system, only a fractional arc of the acceptance ring on the detector mask is needed to be used and the rest of the acceptance ring has to be masked. Several measurements at different arc positions of the acceptance ring should be performed in order to get the whole anisotropic scattering spectrum. In this case, the detector mask selector can be redesigned to accept different parts of acceptance rings.

ACKNOWLEDGMENTS

Constant encouragement from Professor Y. C. Liu is invaluable. This work was supported by the Synchrotron Radiation Research Center and the National Science Council of the Republic of China under Contract Nos. NSC85-2613-M007-001, NSC85-2815-C007-01-001, NSC84-2112-M007-041, and NSC86-2613-M-007-005.

[1] J. M. Schultz and T. C. Long, J. Mater. Sci. **10**, 567 (1975).
[2] J. Bordas and I. H. Munro, Nature (London) **262**, 541 (1976).
[3] J. Bordas, J. Appl. Crystallogr. **11**, 434 (1978).
[4] C. H. Lee, C. S. Hwang, P. K. Tseng, K. L. Yu, H. C. Tseng, W. C. Su, J. R. Chen, T. S. Lin, and S. L. Chang, J. Synchrotron Radiat. **5**, 512 (1998).
[5] W. Shildkamp and C. Pradervand, Rev. Sci. Instrum. **66**, 1956 (1995).
[6] H. H. Jorch and J. L. Campbell, Nucl. Instrum. Methods **143**, 551 (1977).
[7] V. Zobel, J. Eberth, U. Eberth, and E. Eube, Nucl. Instrum. Methods Phys. Res. A **236**, 95 (1985).
[8] C. S. G. Cousins, L. Gerward, D. Laundy, R. E. Meads, J. S. Olsen, and B. J. Sheldon, Nucl. Instrum. Methods Phys. Res. A **324**, 598 (1993).